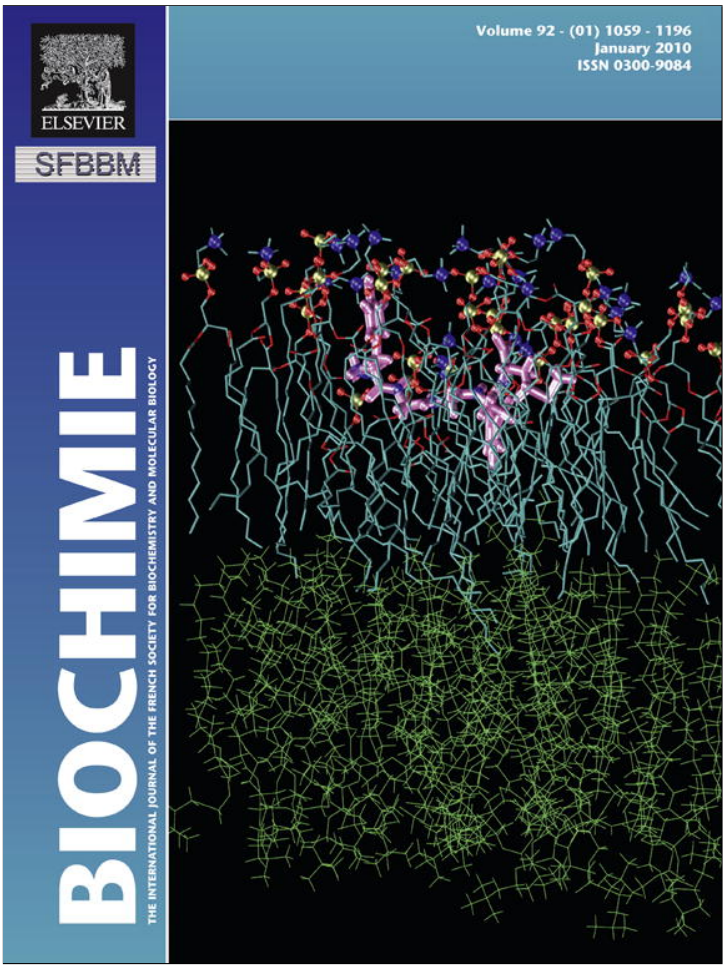

Biochimie 92 (2010) 81–88

Contents lists available at ScienceDirect

Biochimie

journal homepage: www.elsevier.com/locate/biochi

Research paper

Aldose-6-phosphate reductase from apple leaves: Importance of the quaternary structure for enzyme activity

Carlos M. Figueroa, Alberto A. Iglesias*

Laboratorio de Enzimología Molecular, Instituto de Agrobiotecnología del Litoral (UNL–CONICET), Facultad de Bioquímica y Ciencias Biológicas, Paraje "El Pozo" CC 242, S3000ZAA Santa Fe, Argentina

ARTICLE INFO

Article history:
Received 1 June 2009
Accepted 24 September 2009
Available online 30 September 2009

Keywords:
Aldose-6-phosphate reductase
Apple
Carbohydrate metabolism
Glucitol
Sugar-alcohol

ABSTRACT

Aldose-6-phosphate reductase (A6PRase) is a key enzyme for glucitol biosynthesis in plants from the Rosaceae family. To gain on molecular tools for enzymological studies, we developed an accurate system for the heterologous expression of A6PRase from apple leaves. The recombinant enzyme was expressed with a His-tag alternatively placed in the N- or C-terminus, thus allowing the one-step protein purification by immobilized metal affinity chromatography. Both, the N- and the C-term tagged enzymes exhibited similar affinity toward substrates, although the k_{cat} of the latter enzyme was 80-fold lower than that having the His-tag in the N-term. Gel filtration chromatography showed different oligomeric structures arranged by the N- (dimer) and the C-term (monomer) tagged enzymes. These results, reinforced by homology modeling studies, point out the relevance of the C-term domain in the structure of A6PRase to conform an enzyme having optimal specific activity and the proper quaternary structure.

1. Introduction

Certain plants accumulate water-soluble compounds of low molecular weight such as sugar-alcohols, quaternary amines and amino acids [1–3]. These molecules, broadly named compatible solutes, might allow organisms tolerate certain stress conditions by maintaining osmotic balance with the surrounding environment. Particularly, sugar-alcohols are molecules that increase tolerance to oxidative stress [4] and micronutrient deficiency [5]. Glucitol, also called sorbitol, is a sugar-alcohol representing a major photosynthetic end-product in many economically important fruit-bearing tree species from the Rosaceae family, including apple and peach [6,7]. This polyol is the main carbohydrate present in peach leaves [8] and it might serve as anosmoprotectant, as attributed to mannitol in celery [9]. In cells of mature leaves, glucitol is synthesized in the cytosol via reduction of glucose-6-phosphate (Glc6P) to glucitol-6-phosphate (Gol6P) by a NADPH-dependent Glc6P reductase (A6PRase, EC 1.1.1.200) [10,11], followed by hydrolysis of the phosphate group catalyzed by a specific phosphatase (EC 3.1.3.50) [12]. Afterward, the sugar-alcohol is translocated to sink tissues, such as fruits, where it can be metabolized into fructose by a NAD-dependent glucitol dehydrogenase (EC 1.1.1.14) [13].

In plants accumulating sugar-alcohols, photoassimilates partitioning is more complex than in those where sucrose and starch are the two major photosynthetic products. In fact, in the former plants a third compound (a sugar-alcohol) is mainly photosynthesized and accumulated, also representing a major metabolite partitioned within leaf cells as well as between the different non-photosynthetic tissues. Relatively abundant literature is available concerning sucrose and starch metabolism [14–16]; but the regulation of glucitol (and other sugar-alcohols) synthesis and partitioning has been scarcely studied. However, it has been established that in apple leaf discs the expression of the A6PRase gene is enhanced by abscisic acid, low temperature and high salinity [17]. On the other hand, transgenic apple plants with diminished expression of the A6PRase gene showed a switch in leaf carbohydrate content, including reduction of glucitol associated with up-regulation of sucrose [18,19] and starch [19,20] synthesis. Also, tobacco [5] and persimmon [21] plants (which normally do not synthesize polyols) were engineered to produce glucitol by the introduction of the gene coding for apple leaf A6PRase, thus confirming the key role of the enzyme to produce glucitol *in vivo*.

The regulation of glucitol synthesis and degradation is far from being understood, as the enzymes involved in its metabolism have been poorly characterized. Although A6PRases from apple and loquat were purified and their kinetic parameters determined

Abbreviations: A6PRase, aldose-6-phosphate reductase; *Ct*XRase, *Candida tenuis* xylose reductase; Glc6P, glucose-6-phosphate; Gol6P, glucitol-6-phosphate; *Hs*ARase, *Homo sapiens* aldose reductase; IMAC, immobilized metal affinity chromatography; IPTG, isopropyl β-D-1-thiogalactopyranoside; *Md*A6PRase, *Malus domestica* A6PRase.

* Corresponding author. Tel./fax: +54 342 4575206x217.
E-mail address: iglesias@fbcb.unl.edu.ar (A.A. Iglesias).

0300-9084/$ – see front matter © 2009 Elsevier Masson SAS. All rights reserved.
doi:10.1016/j.biochi.2009.09.013

[10,11,22,23], reports about their regulation and structural properties are limited. The absence of convenient systems/protocols for the production of pure protein is a main barrier to advance in the characterization of this plant enzyme. Herein, we report the molecular cloning of the gene that encodes for *Md*A6PRase, its heterologous expression in *Escherichia coli* cells and the simple one-step purification of the recombinant enzyme. To the best of our knowledge, this is the first time that an active A6PRase is successfully expressed in a prokaryotic system.

2. Materials and methods

2.1. Plant material, bacterial strains and media

Fully developed leaves from apple (*Malus domestica*) were obtained from a local farm. Freshly collected leaves were frozen in liquid nitrogen and stored at −80 °C until use. *E. coli* TOP10 (Invitrogen, Carlsbad, CA, USA) cells were used for cloning procedures and plasmid maintenance. Protein expression was carried out with *E. coli* BL21 Star (DE3) (Invitrogen). Cells were grown in LB medium supplemented with ampicillin (100 μg/ml) or kanamycin (50 μg/ml) when necessary.

2.2. RNA extraction, RT-PCR and cloning

Total RNA from apple leaves was isolated as described by Hall et al. [24], and mRNA was purified with the PolyATtract mRNA Isolation System IV (Promega, Madison, WI, USA). cDNA was synthesized at 42 °C for 1 h in a 25 μl reaction mixture containing 0.25 μg mRNA, 200 pmol oligo(dT) primer and 200 U of M-MLV reverse transcriptase (USB, Cleveland, OH, USA). To amplify the gene encoding for A6PRase from apple leaves, we used the specific primers *Md*A6PRase_fw (CATATGTCCACCGTCACCCTGAGCAGTGGC, *Nde*I restriction site is underlined) and *Md*A6PRase_rv (GTCGAC TTATGCATACACGTCTAAGCC, SalI restriction site is underlined) based in the sequence described by Kanayama et al. [25] (GenBank accession no. D11080). The PCR reaction was performed in a 50 μl reaction mixture containing 2 μl cDNA solution, 100 pmol of each primer and 2.5 U *Taq* DNA polymerase (Fermentas, Glen Burnie, MD, USA). PCR conditions were one cycle of 5 min at 95 °C, 30 cycles of 1 min at 95 °C, 30 s at 50 °C and 1 min at 72 °C, followed by a final cycle of 10 min at 72 °C. The amplified gene was cloned into the pGEM-T Easy vector (Promega) and its identity was confirmed by automated sequencing (Macrogen, Seoul, Korea). Sequences were analyzed using the BioEdit Sequence Alignment Editor program [26].

2.3. Protein expression and purification

The gene coding for *Md*A6PRase was subcloned in the expression vectors pET19b and pET24b (Novagen, Madison, WI, USA) to respectively obtain recombinant proteins fused to a His-tag in the N- or C-term. Removal of the stop codon from the gene was necessary prior to subcloning into pET24b to obtain the protein tagged at the C-term. For large scale production of the recombinant enzymes, 1 l of LB medium supplemented with the appropriate antibiotic was inoculated with a 1/100 dilution of an overnight culture of transformed *E. coli* BL21 Star (DE3) cells. The cells were grown at 37 °C in an orbital shaker until OD ~0.6 was reached and then induced overnight with 0.2 mM IPTG at 25 °C. The cells were harvested by centrifugation 15 min at 5000 × *g* and the pellet was frozen at −20 °C until use.

To purify the recombinant proteins, the cells were resuspended in *Buffer A* [25 mM Tris–HCl pH 8.0, 300 mM NaCl, 0.1 mM EDTA, 1 mMβ-mercaptoethanol and 10% (v/v) glycerol] and disrupted by sonication. The resultant suspension was centrifuged 15 min at 10 000 × *g* and the supernatant was loaded in a 5 ml Sepharose-IDA-Ni^{2+} column previously equilibrated with *Buffer A*. The column was washed with 10 bed volumes of *Buffer A* and then with increasing concentrations of imidazole (20, 50, 100 and 250 mM) in *Buffer A* (5 bed volumes each). The recombinant proteins were usually recovered in the fraction containing 250 mM imidazole. The samples were conveniently fractioned and stored at −80 °C in *Buffer A* supplemented with 1 mM EDTA and 0.5 mM DTT. Under these conditions, the recombinant A6PRases were stable for, at least, 6 months.

2.4. Protein determination and SDS-PAGE

Protein concentration was determined after Bradford [27], with BSA utilized as a standard.

Protein electrophoresis under denatured conditions was carried out on discontinuous 12% polyacrylamide gels as described previously [28]. The purity of the enzymes was estimated by densitometry of the stained gels using the program LabImage 2.7 (Kapelan).

2.5. Native molecular mass determination

To determine the molecular mass of the native recombinant proteins, the purified enzymes were subjected to gel filtration chromatography. Samples were loaded in a Superdex 200 HR 10/30 column (Amersham Pharmacia Biotech, Uppsala, Sweden) previously equilibrated with *Buffer B* [25 mM Tris–HCl pH 8.0, 100 mM NaCl and 0.1 mM DTT]. The molecular mass was calculated using the calibration graphic constructed with protein standards.

2.6. Activity assay

Enzyme activity was assayed as described elsewhere [22] with minor modifications. In the direction of Glc6P reduction the standard assay mixture contained 100 mM Tris–HCl pH 8.0, 0.2 mM NADPH and 50 mM Glc6P. In the direction of Gol6P oxidation the standard medium composition was 100 mM Tris–HCl pH 8.0, 1 mM $NADP^+$ and 20 mM Gol6P. Both assays were carried out in a final volume of 50 μl at 25 °C and the oxidation/reduction of NADPH/$NADP^+$ followed using a Multiskan Ascent 384-microplate reader (Thermo Electron Corporation, Waltham, MA, USA). One unit of enzyme activity (U) is defined as the amount of enzyme catalyzing the formation of 1 μmol product ($NADP^+$ or NADPH) in 1 min under the specified assay conditions.

2.7. Kinetic studies

Experimental data of enzyme activity were plotted against variable substrate concentrations and fitted to Hill equation using the program Origin 7.0 (OriginLab Corporation). $S_{0.5}$ is the concentration of substrate giving 50% of the maximal activity (V_{max}). Values of k_{cat} were calculated using V_{max} expressed in U/mg and considering the molecular mass of the enzyme monomer (35 kDa). In inhibition studies, the data were adjusted to a modified Hill equation to obtain the inhibitor concentration which produces 50% of enzyme inhibition ($I_{0.5}$). Kinetic constants ($S_{0.5}$ and k_{cat}) are means of at least two independent sets of data, which were reproducible within ±10%.

2.8. Protein stability and activity with pH and temperature

To evaluate protein stability, the recombinant enzymes were incubated at 25 °C for 10 min at pH values ranging from 6.0 to 10.0. In addition, both enzymes were incubated at pH 8.0 for 10 min at

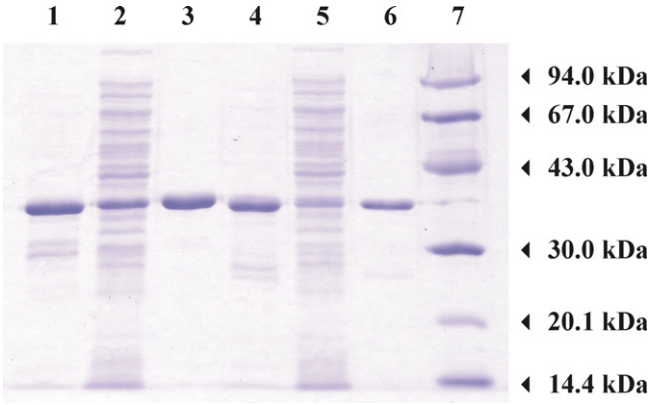

Fig. 1. Analysis of the recombinant proteins by SDS-PAGE. Insoluble and soluble fractions of recombinant cells expressing His-*Md*A6PRase (lanes 1 and 2, respectively) and *Md*A6PRase-His (lanes 4 and 5, respectively). His-*Md*A6PRase and *Md*A6PRase-His purified by IMAC (lanes 3 and 6, respectively). Molecular mass markers (lane 7): 94.0 kDa: phosphorylase β; 67.0 kDa: albumin; 43.0 kDa: ovalbumin; 30.0 kDa: carbonic anhydrase; 20.1 kDa: trypsin inhibitor; 14.4 kDa: α-lactalbumin.

temperatures ranging from 0 to 60 °C. In both assays, an aliquot of the mixture was taken after the treatment to assay enzyme activity in the direction of Glc6P reduction under the standard conditions described above.

The effect of pH and temperature was further evaluated by measuring activity at different values of each of the variables. Thus, the activity of both recombinant proteins was measured in the directions of Glc6P reduction and Gol6P oxidation at pH values ranging from 5.0 to 11.0 and 6.5 to 11.0, respectively. The buffers used were: MES–NaOH (from 5.0 to 6.5), MOPS–NaOH (from 6.5 to 8.0), Tris–HCl (from 8.0 to 9.5) and CAPS–NaOH (from 9.5 to 11.0). Also, activity of Glc6P reduction was measured at pH 8.0 at different temperatures, as specified below.

2.9. Homology modeling

We built a 3D model for A6PRase from apple leaves with the program Modeller 9v2 [29] using the known coordinates of *Candida tenuis* xylose reductase (*Ct*XRase) complexed with NADPH (1K8C) and the crystal structure of *Homo sapiens* aldose reductase (*Hs*ARase) complexed with Glc6P and $NADP^+$ (2ACQ), both available at the Protein Data Bank server (http://www.rcsb.org/pdb/home/home.do). *Ct*XRase (AKR2B5) is a class 2 member of the aldo-keto reductase (AKRase) superfamily [30,31] and its native conformation is a dimer, while *Hs*ARase (AKR1B1) is a class 1 member of the AKRase superfamily [30,31] and its native conformation is a monomer. It has been reported that A6PRases purified from apple seedlings and loquat leaves [10,22] are dimeric and the enzyme from apple leaves has been classified as a class 2 member of the AKRase superfamily (AKR2A1) [30,31]. Therefore, the protein was modeled as a dimer. The accuracy of the model was checked using the Verify3D server (http://nihserver.mbi.ucla.edu/Verify_3D/) [32,33]. Figures were prepared with the Visual Molecular Dynamics (VMD) software (http://www.ks.uiuc.edu/Research/vmd/).

3. Results

3.1. Expression and purification

The gene encoding for A6PRase from apple leaves was successfully amplified and cloned, and the recombinant enzyme was expressed with a His-tag at the N- or C-term using the commercial vectors described under Materials and Methods. SDS-PAGE analysis of crude extracts from the transformed *E. coli* cells showed over-expression of proteins of ~35 kDa (Fig. 1). The A6PRase gene from apple leaves encodes for a putative protein of 310 amino acids (GenBank accession no. BAA01853) with a calculated molecular mass of 34.9 kDa, which is in good agreement with the results showed in Fig. 1. Interestingly, the level of soluble recombinant enzyme was much higher in the N-term tagged protein (His-*Md*A6PRase) than in the C-term tagged one (*Md*A6PRase-His); as in the latter the majority of the protein was found as the insoluble form (Fig. 1). As shown in Fig. 1, the one-step purification protocol allowed us to obtain His-*Md*A6PRase and *Md*A6PRase-His with a level of purity greater than 95% and 75%, respectively. Table 1 shows the results obtained during the purification procedure of both recombinant enzymes. Due to its low soluble expression, the activity of the C-term tagged enzyme was undetectable in crude extracts and a 10-fold concentration was necessary to measure the activity of the purified sample. Table 1 also reports that the amount (both, in terms of protein and activity) of *Md*A6PRase-His obtained after the purification was significantly lower than that of His-*Md*A6Prase. The latter agrees with the low expression of soluble C-term tagged enzyme observed in Fig. 1; but also is a consequence of the almost two order of magnitude difference in specific activity exhibited by the purified recombinant enzymes (see Table 1).

3.2. Structural and kinetic characterization

Seeking to characterize the *Md*A6PRase enzymes His-tagged at the N- or C-term, we determined the kinetic parameters for substrates (data shown in Table 2). The results obtained for His-*Md*A6PRase are very similar to those previously reported for the enzyme purified from apple leaves [11,23] and seedlings [22]. As shown in Table 2, both forms of the recombinant apple enzyme exhibited similar kinetic parameters in terms of $S_{0.5}$ and n_H values for the substrates. However, the *Md*A6PRase-His enzyme showed a remarkable low k_{cat} (and consequently low $k_{cat}/S_{0.5}$ ratios) in both directions of the reaction (Table 2). To find out about possible causes for this unique kinetic difference between the recombinant proteins, their respective quaternary structures were analyzed by gel filtration chromatography. Fig. 2 illustrates that the His-*Md*A6PRase eluted from the Superdex column as a 68 kDa protein, while the *Md*A6PRase-His behaved as a protein of 39 kDa. Considering the theoretical molecular mass of the apple enzyme

Table 1
Purification profiles of the recombinant enzymes.

Enzyme	Step	Volume (ml)	Protein (mg/ml)	Activity (U/ml)	Specific activity (U/mg)	Yield (%)	Purification
His-*Md*A6PRase	Crude extract	27	8.70	1.18	0.136	100	1.0
	IMAC	9.0	2.50	3.13	1.25	88	9.2
*Md*A6PRase-His	IMAC/Conc[a]	0.6	3.09	0.053	0.017	nd[b]	nd

Activity was measured in the reduction of Glc6P direction as described under Materials and methods.
[a] IMAC/Conc.: The protein was concentrated after the purification procedure.
[b] nd: not determined, since no activity was detected in the crude extract of the C-term tagged enzyme.

Table 2
Substrate kinetic parameters for *Md*A6PRase tagged at the N- and C-terminus.

Reaction	Substrate	Parameter	His-*Md*A6PRase	*Md*A6PRase-His
Glc6P reduction		k_{cat} (s^{-1})[a]	0.70 ± 0.02	(9 ± 1) × 10^{-3}
	Glc6P	$S_{0.5}$ (mM)	9.6 ± 0.7	8.1 ± 0.6
		n_H	1.3	1.1
		$k_{cat}/S_{0.5}$ (M^{-1} s^{-1})	73	1.1
	NADPH	$S_{0.5}$ (mM)	0.013 ± 0.001	0.017 ± 0.001
		n_H	1.4	1.9
		$k_{cat}/S_{0.5}$ (M^{-1} s^{-1})	5.4 × 10^4	5.3 × 10^2
Gol6P oxidation		k_{cat} (s^{-1})	0.222 ± 0.006	(1.1 ± 0.2) × 10^{-3}
	Gol6P	$S_{0.5}$ (mM)	3.5 ± 0.3	4.5 ± 0.5
		n_H	1.5	1.0
		$k_{cat}/S_{0.5}$ (M^{-1} s^{-1})	63	0.24
	$NADP^+$	$S_{0.5}$ (mM)	0.019 ± 0.001	0.030 ± 0.006
		n_H	1.2	1.1
		$k_{cat}/S_{0.5}$ (M^{-1} s^{-1})	1.2 × 10^4	37

[a] k_{cat} values were calculated using the molecular mass of the monomer (35 kDa).

(34.9 kDa) and our SDS-PAGE results (Fig. 1), it is concluded that the His-*Md*A6PRase arranges as a dimeric protein; whereas *Md*A6P-Rase-His seems to be a monomer. These results might explain the difference in the kinetic behavior respect to a distinct specific activity that each form of the recombinant enzyme is able to reach.

To evaluate if the tag position could differentially affect protein stability, the recombinant enzymes were incubated for 10 min at different pH values (from pH 6.0 to 10.0) and temperatures (between 0 and 60 °C). As shown in Fig. 3, both enzymes remained fully active in the pH range analyzed; they were stable after incubation below 30 °C, and both similarly inactivated at higher temperatures. Fig. 4 shows pH profiles for the activity determined in both of the reaction directions catalyzed by *Md*A6PRase. Both recombinant enzymes similarly showed optimal activity in a broad pH range in the direction of Glc6P reduction (Fig. 4A), and a narrow range (pH 9.0–10.0) in the opposite oxidative direction (Fig. 4B). These results are similar to those reported for the enzyme purified from apple seedlings [22].

Fig. 5 depicts Arrhenius plots [34] determined for both recombinant enzymes from measurements of the activity in the direction of Glc6P reduction in the range of temperatures where

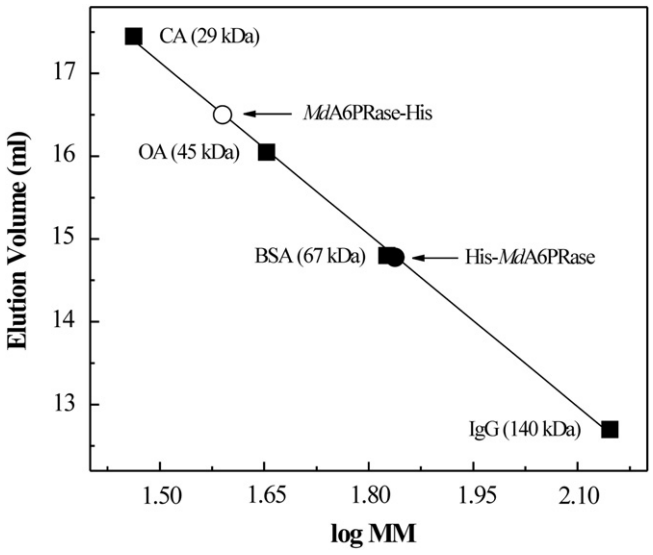

Fig. 2. Gel filtration chromatography in a Superdex 200 HR 10/30 column. Plot of elution volume *vs.* log (molecular mass). (■) Standard proteins: CA (carbonic anhydrase), OA (ovalbumin), BSA and IgG (from equine serum). (●) His-*Md*A6PRase. (○) *Md*A6PRase-His. All the standard proteins were from Sigma–Aldrich (St. Louis, MO, USA), except for IgG that was purified in our laboratory.

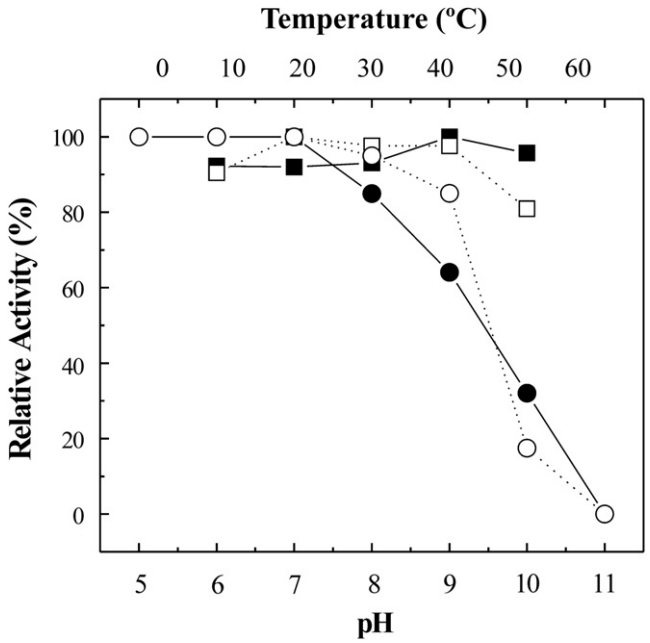

Fig. 3. Analysis of stability for the recombinant proteins. His-*Md*A6PRase (filled symbols) and *Md*A6PRase-His (empty symbols) were incubated 10 min at 25 °C at different pH values (squares) or 10 min at pH 8.0 at different temperatures (circles). After the treatment, the remaining activity was measured in the direction of Glc6P reduction under the standard conditions described in Materials and Methods.

both enzymes were stable (0–30 °C). From the slopes of the lines in Fig. 5, energy of activation (E_a) values of 42.8 kJ mol^{-1} and 12.7 kJ mol^{-1} were calculated for His-*Md*A6PRase and *Md*A6PRase-His, respectively. It is worth considering that the lower E_a was obtained with the form of the recombinant enzyme exhibiting the lower specific activity; thus suggesting that the enzyme containing the His-tag in the C-term thermodynamically favors the accurate formation of the transient activated complex of the reaction [34], even when it exhibits hindrance in promoting products formation.

3.3. Specificity and effectors

The specificity toward the substrates was evaluated using the N-term tagged enzyme. No activity was observed when NADH or NAD^+ was used with Glc6P or Gol6P, respectively. Also, the enzyme utilized Glc6P with high specificity, as this substrate could not be replaced by glucose-1-P, glucose-1,6-bisP, fructose-6-P, fructose-1,6-bisP, fructose-2,6-bisP, mannose-1-P, glucose, galactose, xylose nor by trehalose. Only mannose-6-P could be reduced with NADPH with an enzymatic activity of about 3% of that obtained with Glc6P.

In addition, we analyzed the effect of different metabolites in the activity of His-*Md*A6PRase in the physiological direction of Glc6P reduction. No significant differences were observed when ATP, ADP, AMP, ADP-glucose, UTP, UDP-glucose, Pi or PPi (5 mM each) were added to the enzyme assay mixture. In addition, there were no significant differences in the activity when 10% (v/v) glycerol, 500 mM glucitol or 20% (w/v) sucrose were added to the enzyme assay mixture. However, the inclusion of 200 mM NaCl caused about 65% inhibition of the enzyme activity. A more detailed study showed that different salts were inhibitory, with $I_{0.5}$ values of 120 mM for NaCl, KCl, and NH_4Cl; and of 50 mM for $(NH_4)_2SO_4$. If these results are analyzed in terms of the ionic strength, it is clear that all of the salts exhibit a similar inhibitory pattern.

To evaluate if the inhibition by ionic strength of the His-*Md*A6PRase is caused by disruption of the enzyme quaternary structure, its molecular mass was determined by gel filtration

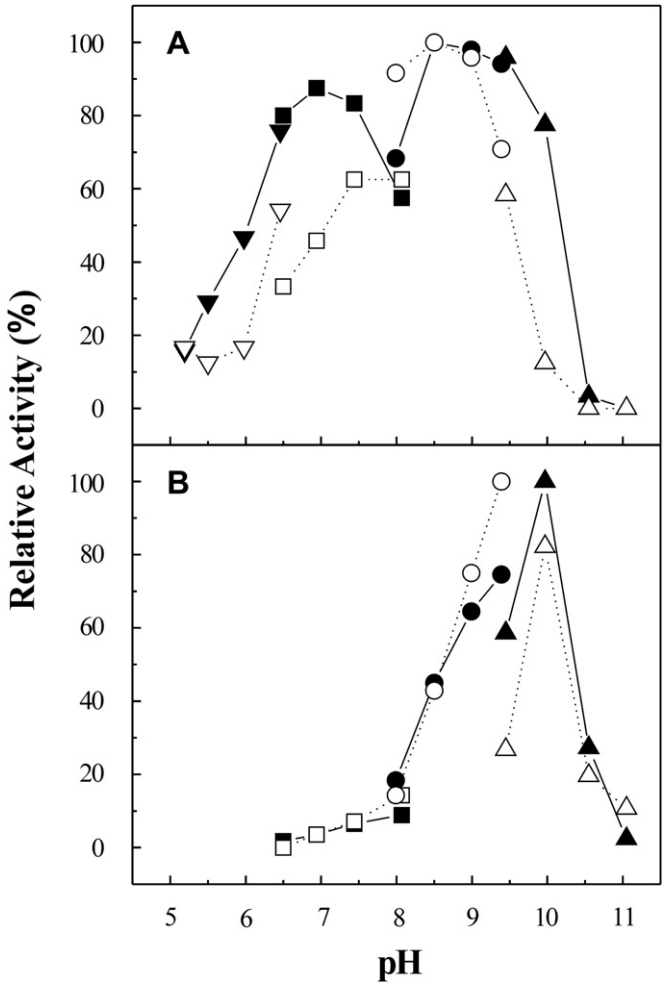

Fig. 4. Enzyme activity of His-*Md*A6PRase (filled symbols) and *Md*A6PRase-His (empty symbols) in the direction of Glc6P reduction (A) and Gol6P oxidation (B) at different pH values. The buffers used were MES-NaOH (down-triangles), MOPS-NaOH (squares), Tris–HCl (circles) and CAPS-NaOH (up-triangles).

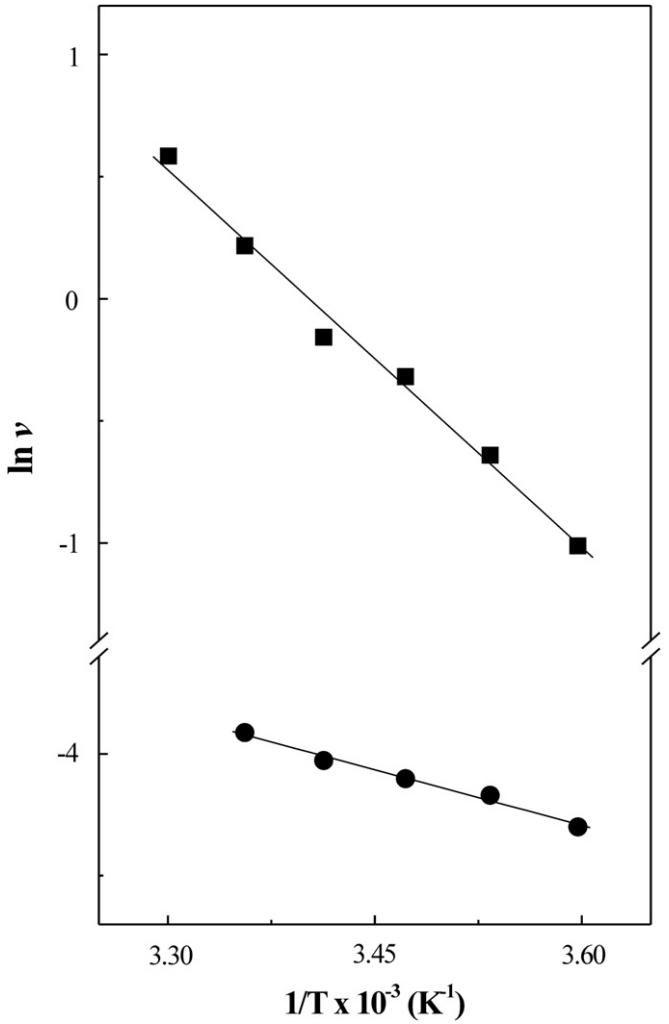

Fig. 5. Arrhenius plots determined for His-*Md*A6PRase (■) and *Md*A6PRase-His (●) from measurements of the activity in the direction of Glc6P reduction in the range were both enzymes were stable (0–30 °C).

chromatography performed with NaCl 500 mM. Under the latter condition, the elution profile of the protein was similar to that obtained at lower levels of the salt (Fig. 2). On the other hand, NaCl also inhibited the monomeric C-term tagged enzyme (see Fig. 2) with an $I_{0.5}$ of 86 mM, thus reinforcing the view that the inhibition of *Md*A6PRase by salts is not forced by dissociation of the enzyme. A further analysis of the inhibition by NaCl revealed that the salt affected the kinetic parameters of the enzyme. Fig. 6 shows how the inclusion of 200 mM NaCl in the assay medium modified the enzyme saturation curves for Glc6P and NADPH. Thus, the salt produced a 2-fold decrease in the V_{max}, and decreased the affinity toward the substrates by about 2.5-fold (Glc6P) and 5-fold (NADPH) (Fig. 6).

3.4. Homology modeling

*Md*A6PRase shares sequence identity of nearly 35% with *Ct*XRase as well as with *Hs*ARase, which is a degree of identity above that necessary to perform molecular modeling accurately [35]. We constructed fifty models of A6PRase from apple leaves utilizing the crystallographic structures of *Ct*XRase and *Hs*ARase as templates with the program Modeller 9v2. The models were evaluated and those ten with the lower *molpdf* values [29] were submitted to the Verify3D server. The model with the best 3D profile is shown in Fig. 7. It can be observed that the protein folds into a $(\beta/\alpha)_8$ barrel, which is the common folding pattern of proteins from the AKRase superfamily [31]. Fig. 7 displays the enzyme complexed with NADPH (inherited from *Ct*XRase, 1K8C) and with Glc6P (inherited from *Hs*ARase, 2ACQ). A detailed analysis of the model shows that both substrates are close to residues Asp43, Tyr48, Lys77 and His108, which are highly conserved among the enzymes of the AKRase superfamily and might be involved in the catalytic mechanism [31,36].

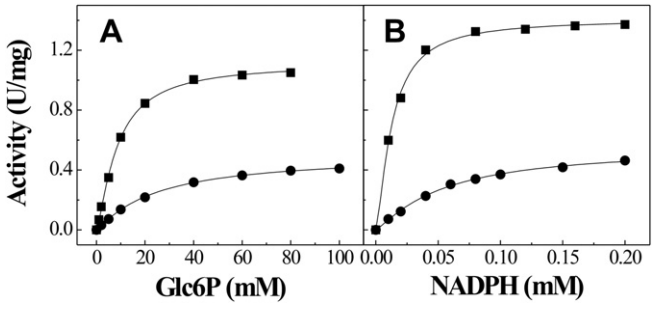

Fig. 6. Effect of NaCl on His-*Md*A6PRase activity. (A) Glc6P curve and (B) NADPH curve in the absence (■) or in the presence of 200 mM NaCl (●).

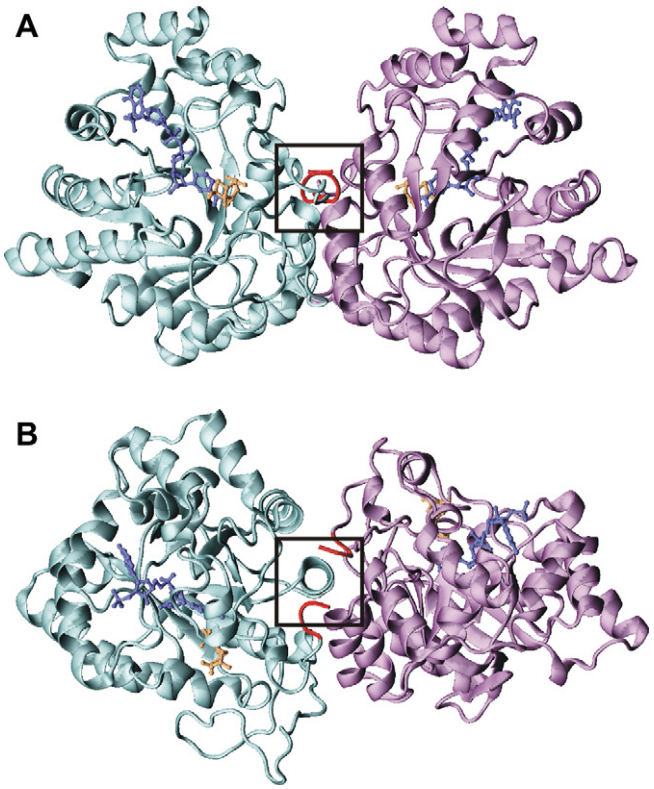

Fig. 7. (A) Homology model of the A6PRase from apple leaves complexed with NADPH (blue) and Glc6P (orange). (B) The model is rotated 90° upside-down. The black boxes are indicating the C-term domain of both subunits (depicted in red).

It has been reported that *Ct*XRase is composed of two subunits that contact each other through residues located in a helix of one chain with residues located at the C-term domain of the other chain [37]. In a remarkable agreement with the latter, the model generated for *Md*A6PRase clearly shows that the C-term domain of each subunit in the dimer is facing to the other one (Fig. 7), which supports that the addition of the tag to this domain might be affecting interactions between subunits, thus making*Md*A6PRase-His to be a monomer, when the recombinant enzyme His-tagged in the N-term forms a dimeric quaternary structure. Remarkably, when we attempted to model the enzyme having the His-tag at the C-term, spatial impediments at the dimer interface were found, resulting in "nonsense" models after inaccuracy for subunits interaction. On the other hand, when the model of His-*Md*A6PRase was built, the tag was oriented to the solvent, thus creating no restriction for the dimer formation (data not shown).

4. Discussion

Several efforts have determined the key role played by A6PRase for glucitol synthesis in plants [5,17–21]. However, little is known about the regulation of this pathway, which is a consequence of the scarce number of studies dedicated to the kinetic characterization of the reductase [10,11,22,23]. In the present work, we have cloned the gene encoding for A6PRase from apple leaves and expressed the recombinant protein in *E. coli* cells to develop an appropriate system for the production of the enzyme with purity required for reliable kinetic and structural characterization. Although the gene had been cloned previously [25], only a short communication describes the recombinant expression of the enzyme fused to the maltose-binding protein [38]. However, it was only used for antibody production rather than been assayed as an active protein.

The enzyme from apple was expressed using two different vectors, which fused a His-tag in the N- or C-term to the recombinant protein, thus producing His-*Md*A6PRase or *Md*A6PRase-His, respectively. The addition of the His-tag was useful for the ease one-step purification by immobilized metal affinity chromatography of the recombinant proteins. The kinetic parameters determined for His-*Md*A6PRase are in good agreement with those reported for the enzyme purified from apple leaves [11,23] and seedlings [22]; which suggest that this form of the enzyme is an accurate tool to be utilized for studies on kinetics and regulation. The latter is not applicable to the recombinant enzyme harboring the His-tag in the C-term. Although both recombinant enzymes exhibited similar apparent affinities for the substrates, they showed significantly different k_{cat} values (and concomitantly $k_{cat}/S_{0.5}$ ratios), being *Md*A6PRase-His a form less active by about two orders of magnitude. Additionally, the latter enzyme was expressed at low levels as a soluble form, which complicates its production in preparative amounts. Altogether, results indicate that the enzyme tagged in the C-term is not a convenient model to produce and characterize leaf A6PRase.

The low specific activity exhibited by *Md*A6PRase-His would not be attributed to affected stability or differences in optimal assay conditions. In fact, the positioning of the His-tag in one or another extreme of the protein caused no effect on enzyme stability in the range of pH 6.0–10.0 and at temperatures below 30 °C. In a same way, both recombinant enzymes showed similar curves of optimal pH in both directions of the catalyzed reaction. Interestingly, measurements of the activity at different temperatures gave Arrhenius plots where the energy of activation (E_a) for *Md*A6PRase-His was lower than that calculated for His-*Md*A6PRase. It may be speculated that the enzyme having a markedly low specific activity (this is *Md*A6PRase-His) is able to efficiently bind substrates ($S_{0.5}$ values are not altered in this enzyme form) and to produce the transient activated complex [34]. The kinetic deficiency for the latter could be due to impediments to convert the activated intermediates into the products or in releasing them to the medium. It may be that this form of the enzyme has an active site with a particular electrostatic and sterical arrangement, which could determine specific dielectric and structural properties for the solvent where the reaction is carried out [39]. A different structure of the active site may induce a slower reaction because the transient activated complex could explore a wider region of phase space that includes essentially nonreactive conformers [40]. The model of a convenient formation of the transition activated complex with a reduced capacity in forming or releasing the products suggests that the enzyme tagged in the C-term would be a good tool to study reaction mechanisms; since it is predicted that it will catalyze the reaction with longer half-life for the activated intermediates, thus with better feasibility for the isolation of them. Also, the kinetic deficiency of *Md*A6PRase-His may be attributed to the fact that a different step in the chemical mechanism of the reaction becomes rate-limiting compared with the enzyme tagged in the N-term [39,40].

The main structural difference between His-*Md*A6PRase and *Md*A6PRase-His was found to be related to the quaternary structure. Thus, the former enzyme was characterized as a dimer (as it was described for the enzyme purified from apple seedlings) [22]; whereas the reductase tagged in the C-term is monomeric. Results support the view that disruption of the dimeric arrangement of the protein affects catalysis, being the main reason for the above discussed markedly distinct k_{cat} exhibited by each recombinant enzyme. These results are highly supported by molecular modeling studies performed for A6PRase utilizing as templates

crystallographic structures of *Ct*XRase and of *Hs*ARase. It has been demonstrated for the resolved structure of the fungal reductase that the C-domain is involved in the aggregation to form a dimer [37], which is consistent with the structure modeled for the apple enzyme, also displaying a key role of the C-term for dimerization. Klimacek and coworkers tried to alter dimer contacts in the fungal xylose reductase by site-directed mutagenesis without success [41]. However, they generated the R180A mutant enzyme, which exhibited a subtle decrease in the k_{cat} compared with that observed for the wild type enzyme, suggesting that the alteration of the dimer interface might have effects in the enzyme activity. The latter is easily associated with the distinctive kinetic and structural properties found for the *Md*A6PRase harboring the His-tag in the C-term. Also supportive were the molecular models we obtained for the enzyme harboring the C-term tag, which revealed 3D steric restrictions for the accurate interaction between subunits.

The N-term tagged enzyme exhibited a high specificity to reversibly catalyze the reduction of Glc6P to Gol6P coupled to the oxidation of NADPH to $NADP^+$; except for mannose-6-P, which is an alternative substrate but the enzyme reaching only 3% of the activity observed with Glc6P. These results are in good agreement with the previously reported data for A6PRase purified from apple and loquat [10,11,22]. On the other hand, the two forms of the recombinant enzyme were inhibited by high ionic strength in the assay medium. The inhibition was not caused by changes in the quaternary structure, but high concentrations of salts provoked a decrease in V_{max} and an increase in the $S_{0.5}$. The rationale for the inhibitory effect seems to be that the increase of ionic strength disrupts the conditions in the environment where the substrates bind to the enzyme and where catalysis takes place. The fact that the substrates are ionic molecules logically supports this view.

5. Concluding remarks

We present, for the first time, the recombinant expression of an active A6PRase in a prokaryotic system. The one-step purification procedure of the N-term tagged enzyme seems to be an accurate method for the production of preparative amounts of A6PRasefor kinetic and structural analysis. Also, we provided evidence for the importance of the recombinant A6PRase from apple leaves C-term to obtain the optimal specific activity and the appropriate quaternary structure. Therefore, these results represent a promising tool to advance in the characterization of structure to function relationships in A6PRase. Such work is currently in progress.

Acknowledgments

This work was supported in part by Consejo Nacional de Investigaciones Científicas y Técnicas (CONICET, PIP 6358), Agencia Nacional de Promoción Científica y Tecnológica (ANPCyT, PICTO'05 15-36129) and Universidad Nacional del Litoral (UNL, CAI+D 2006). C.M.F. is a Postdoctoral Fellow and A.A.I. is a member of the Researcher Career from CONICET.

References

[1] H.J. Bohnert, R.G. Jensen, Strategies for engineering water-stress tolerance in plants. Trends Biotechnol. 14 (1996) 89–97.
[2] N. Smirnoff, Plant resistance to environmental stress. Curr. Opin. Biotechnol. 9 (1998) 214–219.
[3] W. Loescher, J. Everard, Regulation of sugar alcohol biosynthesis. in: R.C. Leegood, T.D. Sharkey, S. von Caemmerer (Eds.), Photosynthesis: Physiology and Metabolism. Kluwer Academic Publishers, Dordrecht, 2000, pp. 275–299.
[4] B. Shen, R.G. Jensen, H.J. Bohnert, Increased resistance to oxidative stress in transgenic plants by targeting mannitol biosynthesis to chloroplasts. Plant Physiol. 113 (1997) 1177–1183.
[5] P.H. Brown, N. Bellaloui, H. Hu, A. Dandekar, Transgenically enhanced sorbitol synthesis facilitates phloem boron transport and increases tolerance of tobacco to boron deficiency. Plant Physiol. 119 (1999) 17–20.
[6] C.R. Grant, T. ap Rees, Sorbitol metabolism by apple seedlings. Phytochemistry 20 (1981) 1505–1511.
[7] A. Moing, F. Carbonne, M.H. Rashad, J.P. Gaudillere, Carbon fluxes in mature peach leaves. Plant Physiol. 100 (1992) 1878–1884.
[8] J. Nadwodnik, G. Lohaus, Subcellular concentrations of sugar alcohols and sugars in relation to phloem translocation in *Plantago major*, *Plantago maritima*, *Prunus persica*, and *Apium graveolens*. Planta 227 (2008) 1079–1089.
[9] D.M. Pharr, J.M.H. Stoop, J.D. Williamson, M.E.S. Feusi, M.O. Massel, M.A. Conkling, The dual role of mannitol as osmoprotectant and photoassimilate in celery. HortScience 30 (1995) 1182–1188.
[10] M. Hirai, Purification and characteristics of sorbitol-6-phosphate dehydrogenase from loquat leaves. Plant Physiol. 67 (1981) 221–224.
[11] F.B. Negm, W.H. Loescher, Characterization and partial purification of aldose-6-phosphate reductase (alditol-6-phosphate:NADP 1-oxidoreductase) from apple leaves. Plant Physiol. 67 (1981) 139–142.
[12] R. Zhou, L. Cheng, R. Wayne, Purification and characterization of sorbitol-6-phosphate phosphatase from apple leaves. Plant Sci. 165 (2003) 227–232.
[13] J. Berüter, M.E.S. Feusi, The effect of girdling on carbohydrate partitioning in the growing apple fruit. J. Plant Physiol. 151 (1997) 277–285.
[14] M.A. Ballicora, A.A. Iglesias, J. Preiss, ADP-glucose pyrophosphorylase: a regulatory enzyme for plant starch synthesis. Photosynth. Res. 79 (2004) 1–24.
[15] A.A. Iglesias, F.E. Podestá, Photosynthate formation and partitioning in crop plants. in: M. Pessarakli (Ed.), Handbook of Photosynthesis. CRC Press, Boca Raton, 2005, pp. 525–545.
[16] H. Winter, S.C. Huber, Regulation of sucrose metabolism in higher plants: localization and regulation of activity of key enzymes. Crit. Rev. Biochem. Mol. Biol. 35 (2000) 253–289.
[17] Y. Kanayama, M. Watanabe, R. Moriguchi, M. Deguchi, K. Kanahama, S. Yamaki, Effects of low temperature and abscisic acid on the expression of the sorbitol-6-phosphate dehydrogenase gene in apple leaves. J. Japan. Soc. Hort. Sci. 75 (2006) 20–25.
[18] N. Kanamaru, Y. Ito, S. Komori, M. Saito, H. Kato, S. Takahashi, M. Omura, J. Soejima, K. Shiratake, K. Yamada, S. Yamaki, Transgenic apple transformed by sorbitol-6-phosphate dehydrogenase cDNA: switch between sorbitol and sucrose supply due to its gene expression. Plant Sci. 167 (2004) 55–61.
[19] G. Teo, Y. Suzuki, S.L. Uratsu, B. Lampinen, N. Ormonde, W.K. Hu, T.M. DeJong, A.M. Dandekar, Silencing leaf sorbitol synthesis alters long-distance partitioning and apple fruit quality. Proc. Natl. Acad. Sci. U.S.A. 103 (2006) 18842–18847.
[20] L. Cheng, R. Zhou, E.J. Reidel, T.D. Sharkey, A.M. Dandekar, Antisense inhibition of sorbitol synthesis leads to up-regulation of starch synthesis without altering CO_2 assimilation in apple leaves. Planta 220 (2005) 767–776.
[21] M. Gao, R. Tao, K. Miura, A.M. Dandekar, A. Sugiura, Transformation of Japanese persimmon (*Diospyros kaki* Thunb.) with apple cDNA encoding NADP-dependent sorbitol-6-phosphate dehydrogenase. Plant Sci. 160 (2001) 837–845.
[22] Y. Kanayama, S. Yamaki, Purification and properties of NADP-dependent sorbitol-6-phosphate dehydrogenase from apple seedlings. Plant Cell Physiol. 34 (1993) 819–823.
[23] R. Zhou, R.C. Sicher, L. Cheng, B. Quebedeaux, Regulation of apple leaf aldose-6-phosphate reductase activity by inorganic phosphate and divalent cations. Funct. Plant Biol. 30 (2003) 1037–1043.
[24] T.C. Hall, Y. Ma, B.U. Buchbinder, J.W. Pyne, S.M. Sun, F.A. Bliss, Messenger RNA for G1 protein of French bean seeds: cell-free translation and product characterization. Proc. Natl. Acad. Sci. U.S.A. 75 (1978) 3196–3200.
[25] Y. Kanayama, H. Mori, H. Imaseki, S. Yamaki, Nucleotide sequence of a cDNA encoding NADP-sorbitol-6-phosphate dehydrogenase from apple. Plant Physiol. 100 (1992) 1607–1608.
[26] T.A. Hall, BioEdit: a user-friendly biological sequence alignment editor and analysis program for Windows 95/98/NT. Nucl. Acids Symp. Ser. 41 (1999) 95–98.
[27] M.M. Bradford, A rapid and sensitive method for the quantitation of microgram quantities of protein utilizing the principle of protein-dye binding. Anal. Biochem. 72 (1976) 248–254.
[28] U.K. Laemmli, Cleavage of structural proteins during the assembly of the head of bacteriophage T4. Nature 227 (1970) 680–685.
[29] A. Sali, T.L. Blundell, Comparative protein modelling by satisfaction of spatial restraints. J. Mol. Biol. 234 (1993) 779–815.
[30] D. Hyndman, D.R. Bauman, V.V. Heredia, T.M. Penning, The aldo-keto reductase superfamily homepage. Chem. Biol. Interact. 143-144 (2003) 621–631.
[31] J.M. Jez, M.J. Bennett, B.P. Schlegel, M. Lewis, T.M. Penning, Comparative anatomy of the aldo-keto reductase superfamily. Biochem. J. 326 (Pt 3) (1997) 625–636.
[32] J.U. Bowie, R. Luthy, D. Eisenberg, A method to identify protein sequences that fold into a known three-dimensional structure. Science 253 (1991) 164–170.
[33] R. Luthy, J.U. Bowie, D. Eisenberg, Assessment of protein models with three-dimensional profiles. Nature 356 (1992) 83–85.

[34] I.H. Segel, Enzyme Kinetics. Behavior and Analysis of Rapid Equilibrium and Steady-State Enzyme Systems. Wiley-Interscience, New York, 1993.
[35] K. Ginalski, Comparative modeling for protein structure prediction. Curr. Opin. Struct. Biol. 16 (2006) 172–177.
[36] R. Kratzer, D.K. Wilson, B. Nidetzky, Catalytic mechanism and substrate selectivity of aldo-keto reductases: insights from structure-function studies of *Candida tenuis* xylose reductase. IUBMB Life 58 (2006) 499–507.
[37] K.L. Kavanagh, M. Klimacek, B. Nidetzky, D.K. Wilson, The structure of apo and holo forms of xylose reductase, a dimeric aldo-keto reductase from *Candida tenuis*. Biochemistry 41 (2002) 8785–8795.
[38] Y. Kanayama, K. Sakanishi, H. Mori, S. Yamaki, Expression of the gene for NADP-dependent sorbitol-6-phosphate dehydrogenase in apple seedlings. Plant Cell Physiol. 36 (1995) 1139–1141.
[39] T.C. Bruice, S.J. Benkovic, Chemical basis for enzyme catalysis. Biochemistry 39 (2000) 6267–6274.
[40] D. Truhlar, A. Kohen, Convex Arrhenius plots and their interpretation. Proc. Natl. Acad. Sci. U.S.A. 98 (2001) 848–851.
[41] M. Klimacek, F. Wuhrer, K.L. Kavanagh, D.K. Wilson, B. Nidetzky, Altering dimer contacts in xylose reductase from *Candida tenuis* by site-directed mutagenesis: structural and functional properties of R180A mutant. Chem. Biol. Interact. 143–144 (2003) 523–532.